

## 4.1 ENHANCED CLIMATIC WARMING OVER THE TIBETAN PLATEAU DUE TO DOUBLING CO<sub>2</sub>: A MODEL STUDY

Baode Chen\*

GEST Center, University of Maryland, Baltimore County, Maryland

Winston C. Chao

NASA/Goddard Space Flight Center, Greenbelt, Maryland

Xiaodong Liu

Institute of Earth Environment, CAS, Xian, China

### 1. INTRODUCTION

A number of studies have presented the evidences that surface climate change associated with global warming at high elevation sites shows more pronounced warming than at low elevations, i.e. an elevation dependency of climatic warming (e.g. Beniston et al., 1997). Giorgi et al. (1997) pointed out that snow-albedo feedback may be responsible for the excessive warming in the Swiss Alps. From an ensemble of climate change experiments of increasing greenhouse gases and aerosols using an air-sea coupled climate model, Fyfe and Flato (1999) found a marked elevation dependency of the simulated surface screen temperature increase over the Rocky Mountains.

Using almost all available instrumental records, Liu and Chen (2000) showed that the main portion of the Tibetan Plateau (TP) has experienced significant ground temperature warming since the mid-1950s, especially in winter, and that there is a tendency for the warming trend to increase with elevation in the TP as well as its surrounding areas. In this paper, we will investigate the mechanism of elevation dependency of climatic warming in the TP by using a high-resolution regional climate model.

### 2. THE MODEL AND EXPERIMENT DESIGN

The latest version of the National Center for Atmospheric Research (NCAR) region climate model version 2 (RegCM2) is used. An area covering the entire TP was selected for our purpose. A 60 km grid size and 14 levels with the model top at 80 hPa are used. Two 1-year runs have been carried out with time-dependent lateral meteorological field provided by a 130-year transient increasing CO<sub>2</sub> simulation of the NCAR Climate System Model (CSM) (Meehl et al, 2000). From the 130-year CSM simulation, one year is selected as the control run when CO<sub>2</sub> level being held at the present day value

(355 ppm) and another as the 2XCO<sub>2</sub> run when doubling CO<sub>2</sub> being achieved.

### 3. THE ENHANCED CLIMATIC WARMING SIGNAL DETECTED FROM THE EXPERIMENTS

The ground temperature difference between RegCM2 2XCO<sub>2</sub> and control run are plotted in Fig. 1 as a function of elevation over the model grid points for summer, winter and annual means. In Fig. 1, topographical elevation is grouped into 10 categories with a 500-m interval, i.e., 0.5 - 1.0 km, 1.0-1.5 km,...,5.0-5.5 km, and the value of temperature difference is obtained by averaging results over all grid points in each elevation category. The number of grid points used in the averaging for each elevation category varies from a maximum of 895 for 0.5-1.0 km category to a minimum of 69 for elevation between 3.5-4.0 km.

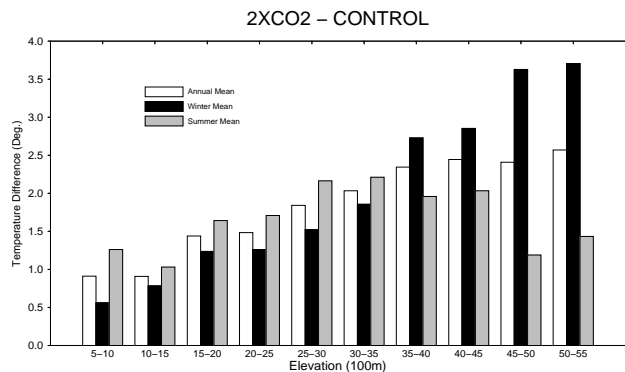


Fig.1: Ground temperature difference between 2 X CO<sub>2</sub> and control run as a function of elevation

The annually averaged warming is from 0.9°C at the lowest elevation to 2.6°C at the highest sites. Considering the CSM shows a relatively weak sensitivity to CO<sub>2</sub> concentration (e.g. Meehl et al, 2000) and a relatively large sample size to produce average, the simulated warming is quite profound around the TP.

A remarkable tendency of warming increasing with elevation can be found for winter season. The maximum temperature increase is 3.7°C at 4.5 to 5.5 km elevation, and the warming is 3.1°C more than that at 0.5 to 1.0 km. For summer the elevation dependency

\*Corresponding author address: Baode Chen, GEST Center, NASA/Goddard Space Flight Center, Code 913, Greenbelt, MD 20771; e-mail: bdchen@climate.gsfc.nasa.gov.

is not clearly recognized. It can be seen that there is a maximum of  $2.2^{\circ}\text{C}$  warming at 2.5-3.0 km and weaker warming below or above. This result is consistent with Liu and Chen's observational study (2001).

#### 4. SURFACE ENERGY BUDGET

Fig. 2 shows the differences between  $2\text{XCO}_2$  and control run net solar radiative flux plus downward longwave flux at surface ( $S_g + F_{IR} \downarrow$ ), infrared radiation flux emitted from the surface ( $\sigma T_s^4$ ), surface sensible heating flux and latent heating flux as a function of elevation for winter. It can be seen that the ( $S_g + F_{IR} \downarrow$ ) displays a strong increase with elevation in the  $2\text{XCO}_2$  run, which is mostly responsible for elevation dependence of the ground temperature. There is a very weak elevation signal found in the  $2\text{XCO}_2$  -Control run latent heating flux between 5-10 km and 45-50 km, and fluctuation is evident in the sensible heating flux.

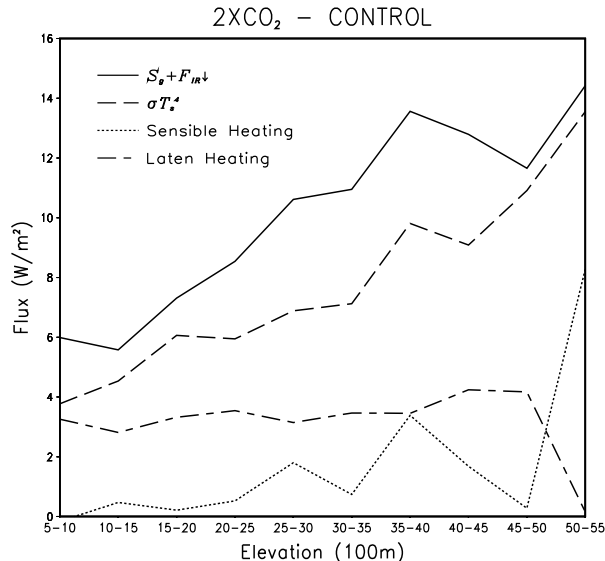


Fig.2: Difference between  $2\text{XCO}_2$  and control run surface fluxes as a function of elevation for the winter season.

The differences between  $2\text{XCO}_2$  and control run absorbed solar flux  $S_g$  as well as downward longwave flux  $F_{IR} \downarrow$  are illustrated in Fig. 3. The absorbed solar flux shows a decline for the  $2\text{XCO}_2$  run in an elevation range of 5km to 25 km and the decrease becomes weaker as elevation increasing. In the  $2\text{XCO}_2$  run the stronger enhancement of precipitation (not shown) is found at the lower elevations from 5km to 25 km height, indicating an increase in clouds which will result in a larger decrease in solar flux reaching the surface. Large snow depletion (not shown) is detected at elevations between 25 km to 40 km in the  $2\text{XCO}_2$  run, as a result of snow depletion which leads to a decrease in albedo, and more

solar flux is absorbed at the surface. On the other hand, because of the "greenhouse effect" resulted from doubling  $\text{CO}_2$ , the downward longwave flux at the surface is enhanced as shown in Fig. 3, and the enhancement appears to be stronger at higher elevations, in particular, in the range of 30 km to 50 km. The combination of these effects will produce an elevation dependency in the ( $S_g + F_{IR} \downarrow$ ) which results in enhanced warming over the Tibetan Plateau.

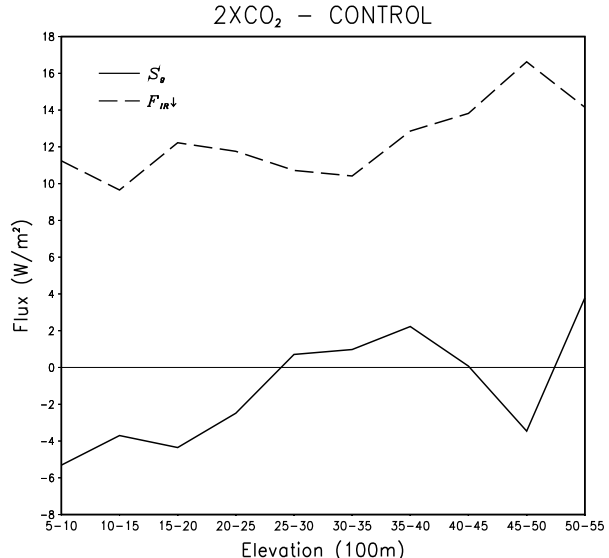


Fig.3: Difference between  $2\text{XCO}_2$  and control run absorbed solar flux  $S_g$  and downward longwave flux  $F_{IR} \downarrow$  at the surface as a function of elevation for the winter season

**Acknowledgments.** The authors would like to thank Drs. J. Qian and X. Bi for providing the model code and data. This work was supported by NASA/Office of Earth Sciences. XD Liu also thanks for the support from Chinese Academy of Sciences.

#### 5. REFERENCES

- Beniston, M., M. Diaz and R. S. Bradley, 1997: Climatic change at high elevation sites: an overview. *Climatic Change*, **36**, 1060-1622.
- Fyfe, J. C. and G. M. Flato, 1999: Enhanced climatic change and its detection over the Rocky mountains. *J. Climate*, **12**, 230 - 243.
- Giorgi, F, J . W. Hurrell, M. R. Marinucci and M. Beniston, 1997: Elevation dependency of the surface climate change signal: a model study. *J. Climate*, **10**, 288 - 296.
- Liu, X. D. and B. Chen, 2000: Climatic Warming in the Tibetan Plateau during recent decades. *Int. J. of Climatology*, **20**, 1729 - 1742.